



Cite this: *Dalton Trans.*, 2018, **47**, 15024

Received 18th September 2018,  
Accepted 29th September 2018

DOI: 10.1039/c8dt03780a

rsc.li/dalton

## Copper(II) complexes for cysteine detection using $^{19}\text{F}$ magnetic resonance†

José S. Enriquez,  Meng Yu,  Bailey S. Bouley,  Da Xie  and Emily L. Que \*

Cysteine plays an essential role in maintaining cellular redox homeostasis and perturbations in cysteine concentration are associated with cardiovascular disease, liver disease, and cancer.  $^{19}\text{F}$  MRI is a promising modality for detecting cysteine in biology due to its high tissue penetration and negligible biological background signal. Herein we report fluorinated macrocyclic copper complexes that display a  $^{19}\text{F}$  NMR/MRI turn-on response following reduction of the Cu(II) complexes by cysteine. The reactivity with cysteine was studied by monitoring the appearance of a robust diamagnetic  $^{19}\text{F}$  signal following addition of cysteine in conjunction with UV-vis and EPR spectroscopies. Importantly, complexes with  $-\text{CH}_2\text{CF}_3$  tags display good water solubility. Studies with this complex in HeLa cells demonstrate the applicability of these probes to detect cysteine in complex biological environments.

### Introduction

Cysteine is an essential amino acid that plays an important role in the regulation of a range of cellular processes related to redox homeostasis.<sup>1,2</sup> It is involved in the synthesis of glutathione (GSH),<sup>3</sup> an important tripeptide that is an abundant intracellular redox buffer, and is a well-known bio-reductant alongside GSH, NADH, and HNO.<sup>4</sup> The intracellular concentration of cysteine varies from 30 to 200  $\mu\text{M}$  depending on the cell type.<sup>5–7</sup> Perturbations in the concentration of cysteine are associated with pathologies including cardiovascular disease, liver disease, and cancer.<sup>8,9</sup>

The important role of cysteine in both health and disease has led to the development of probes to detect and monitor its intracellular levels.<sup>10–12</sup> Many of these probes rely on fluorescence to track cysteine at the cellular level.<sup>6,13–19</sup> However, translating these studies into animal models is limited by the poor penetration depth of fluorescence microscopy. Other common strategies for detecting cysteine include colorimetric and electrochemical methods,<sup>14,20–27</sup> however, these methods are difficult to translate into cellular and animal models.

In this study, we developed two novel probes to track cysteine using Magnetic Resonance Imaging (MRI), a non-invasive diagnostic imaging modality with high penetration depth. Currently, clinical MRI is used to detect protons ( $^1\text{H}$ ), but due to the abundance of protons in biological systems,

$^1\text{H}$  MR images have high and heterogeneous background signal that complicate the use of sensors in this modality.<sup>28–30</sup>

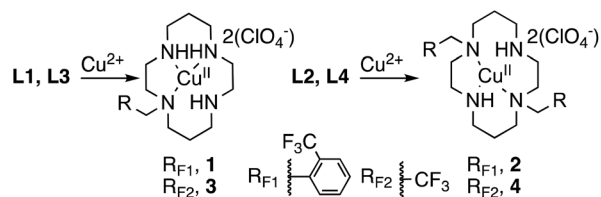
A promising alternative is  $^{19}\text{F}$  MRI as there is a negligible amount of detectable fluorine in the body, resulting in zero biological background signal. Further,  $^{19}\text{F}$  has favorable NMR characteristics including a similar gyromagnetic ratio to  $^1\text{H}$ , a nuclear spin of  $\frac{1}{2}$ , and a comparable sensitivity: 83% relative to that of proton.<sup>30,31</sup> Paramagnetic metal centers can be used to modulate  $^{19}\text{F}$  signal, which has been exploited in a number of transition metal and lanthanide complexes.<sup>32–44</sup>

Our  $^{19}\text{F}$  MR sensor platforms contain Cu(II) owing to its ability to be reduced by bioreductants and act as an “off-on” switch for  $^{19}\text{F}$  signals. Copper has two common oxidation states that have distinct magnetic properties: Cu(II) is paramagnetic while Cu(I) is diamagnetic, and both oxidation states are accessible in biological systems. In the Cu(II) oxidation state, the paramagnetic center will silence the fluorine signal *via* paramagnetic relaxation enhancement (PRE).<sup>35,45</sup> The long electronic relaxation time of Cu(II) results in drastic reduction in  $T_1$  and  $T_2$  relaxation times. Lowering  $T_2$  can cause severe line broadening, effectively quenching the  $^{19}\text{F}$  signal.<sup>46</sup> By careful tuning of the ligand environment, the Cu(II) can be reduced to Cu(I) by a bioreductant of choice, in this case cysteine. This reduction is accompanied by an increase in  $^{19}\text{F}$   $T_1$  and  $T_2$  and a reappearance of the  $^{19}\text{F}$  signal, which can be detected by both NMR and MRI. We have been able to exploit a similar mechanism to develop Cu(II) based  $^{19}\text{F}$  MRI probes for hypoxia.<sup>33,34</sup>

To make a cysteine-responsive Cu(II) complex, cyclam (1,4,8,11-tetraazacyclotetradecane) was chosen as a favorable ligand scaffold owing to its high binding affinity towards Cu(II) ( $\text{p}K_{\text{d}} \approx 25$ ).<sup>47</sup> Addition of aromatic or alkyl substituents on the

Department of Chemistry, The University of Texas at Austin, 105 E. 24th St Stop A5300, Austin, Texas 78712, USA. E-mail: emilyque@cm.utexas.edu

† Electronic supplementary information (ESI) available. CCDC 1851180–1851182. For ESI and crystallographic data in CIF or other electronic format see DOI: 10.1039/c8dt03780a



Scheme 1 Structures of Cu(II) complexes 1–4.

macrocyclic ring can shift the  $E_{1/2}$  of Cu(II)/Cu(I) cathodically which renders the Cu(II) complex more prone to reduction by weaker reductants like cysteine: an idea that has been demonstrated by some reported NO or HNO fluorescence sensors.<sup>48,49</sup> Based on this strategy, four different ligands and their corresponding Cu(II) complexes were synthesized containing either fluorinated benzyl (1, 2) or alkyl substituents (3, 4) (Scheme 1). 1,8-Disubstituted cyclam complexes 2 and 4 displayed robust turn-on responses in the presence of 3 equivalents of cysteine. Improved water solubility was observed for alkyl-substituted 4, consistent with previously reported Ni(II) analogues.<sup>50,51</sup> Response of these probes to cysteine in solution is described along with the application of water-soluble 4 for the detection of cysteine in mammalian cell lines.

## Results and discussion

### Synthesis

Ligand L1 was readily synthesized in 60% yield by a one-step reaction between cyclam and 2-trifluoromethylbenzyl bromide. Di-substituted ligand L2 was obtained by reaction between bis-formyl cyclam and two equivalents of 2-trifluoromethylbenzyl bromide, followed by base-mediated hydrolysis to yield the desired product in 40% overall yield over three steps. Ligand L3 was synthesized by protecting cyclam with benzyl bromide to form the tris alkylated species and reacting with trifluoroacetic anhydride. Following reduction of the carbonyl to a

methylene and removal of the benzyl protecting group, ligand L3 was furnished. Ligand L4 was synthesized using a modified literature procedure.<sup>51</sup> Copper complexes 1, 2, 3, and 4 were synthesized by combining ligand and Cu(ClO<sub>4</sub>)<sub>2</sub> in methanol, and purified by washing the resulting purple precipitate with diethyl ether or by the use of reverse-phase chromatography. Complete synthetic schemes are shown in the ESI.†

### Solid state structural characterization

Single crystals suitable for X-ray diffraction were obtained by slow evaporation of CH<sub>3</sub>CN/H<sub>2</sub>O (3 : 7) solutions of 1, 2, and 4 (Fig. 1). No X-ray quality crystals of 3 could be obtained. All crystal structures reveal distorted octahedral geometries at the Cu centers with four nitrogen atoms occupying the equatorial plane and two oxygen atoms from perchlorate counter ions in the axial positions. All three structures display a *trans*-III configuration with two adjacent N–R groups of the macrocycle (R = H or the alkyl group) pointing towards one side of the cyclam plane while the other two pointing to the opposite side.<sup>52</sup> As expected, the introduction of trifluorobenzyl or trifluoromethyl groups on the nitrogen atoms results in Cu–N bond elongation (0.1 Å) compared to the other Cu–N bonds. The Cu–F average distances were 5–6 Å for complexes 1, 2, and 4, well within the range for the PRE effect.<sup>45</sup>

### Solution state characterization

**UV-Vis spectroscopy.** The UV-vis spectrum of 1 displays a d–d transition band at 530 nm ( $\epsilon = 220 \text{ M}^{-1} \text{ cm}^{-1}$ , Fig. S1†) in HEPES/CH<sub>3</sub>CN solution (HEPES: 50 mM, pH 7.2, NaCl 0.1 M; HEPES : CH<sub>3</sub>CN = 6 : 4 v/v). Complex 2 exhibits an analogous absorption feature at 563 nm ( $\epsilon = 384 \text{ M}^{-1} \text{ cm}^{-1}$ , Fig. S1†). Complex 3 in HEPES buffer displays a d–d transition at 537 nm ( $\epsilon = 124 \text{ M}^{-1} \text{ cm}^{-1}$ ) and complex 4 displays an absorption feature at 548 nm ( $\epsilon = 212 \text{ M}^{-1} \text{ cm}^{-1}$ ) (Fig. S1†). These values are comparable to those reported for tetracoordinate cyclam copper(II) complexes with square-planar geometry.<sup>53</sup>

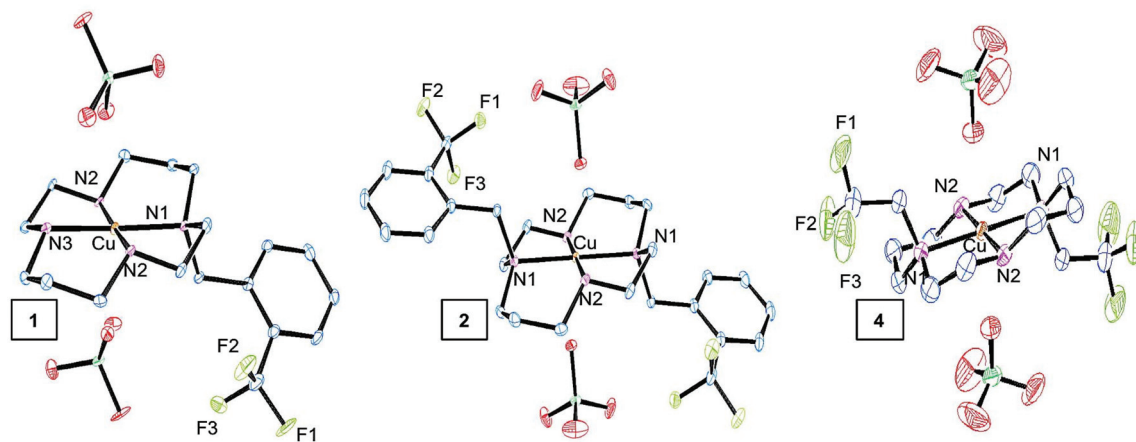


Fig. 1 ORTEP drawing of 1, 2, and 4; the thermal ellipsoids are at the 50% probability level. Blue: carbon, purple: nitrogen, light green: fluorine, orange: copper, red: oxygen and dark green: chlorine.

**Cyclic voltammetry.** In DMF solution, complex **1** gave a quasi-reversible feature with  $E_{1/2} = -1.04$  V (vs. ferrocene,  $\Delta E = 226$  mV) which was assigned to the Cu(I)/Cu(II) redox couple (Fig. S2†). A similar feature was observed in complex **2** with a more positive redox potential  $E_{1/2} = -0.74$  V ( $\Delta E = 117$  mV). Introduction of a second trifluoromethylbenzyl ring shifts the redox potential positively by 300 mV. For reference, we synthesized the Cu(II) complex of 1,8-dibenzyl cyclam (**5**) and found that the redox potential is more negative ( $E_{1/2} = -0.93$  V), indicating that the incorporation of CF<sub>3</sub> groups plays a role in positively shifting the redox potential in our system. In addition, the position of the CF<sub>3</sub> group is important. When the CF<sub>3</sub> is placed at the *para*-position instead of the *ortho*-position (**6**), a redox potential of  $-0.88$  V was observed. Compared to complex **2**, a 140 mV negative shift was observed, most likely due to weakened inductive effect of the *para* vs. *ortho* CF<sub>3</sub> groups. Under the same conditions, complex **3** gives a feature at  $E_{1/2} = -0.96$  V ( $\Delta E = 400$  mV) and complex **4** gives a quasi-reversible feature at  $E_{1/2} = -0.74$  V ( $\Delta E = 127$  mV), which are comparable with the benzyl systems. Moreover, an irreversible oxidation peak was observed in all complexes **1–4** with  $E^{\circ} = -0.24$  V,  $-0.38$  V,  $-0.12$  V, and  $-0.23$  V, respectively. This feature is reminiscent of the redox behavior in the Cu(II) complex of tetramethylcyclam (TMC) and has been attributed to the rapid structural reorganization or isomerization of the Cu(I) *trans*-III intermediate in the TMC system.<sup>54</sup>

### Cysteine reactivity

In order to investigate the reactivity of complexes **1–4** towards cysteine, we monitored the disappearance of the Cu(II) d-d absorbance band using UV-Vis. Complexes **1** and **3** show limited reactivity towards cysteine. For complex **1**, only 43% reduction in the d-d band was observed after 40 min in the

presence of 12 equivalents of cysteine. For complex **3**, only 55% reduction was observed after 10 minutes in the presence of 9 equivalents of cysteine (Fig. S3†). Conversely, reaction of complexes **2** and **4** with cysteine was rapid and associated with a color change from purple to colorless (Fig. 2). For complex **2**, based on the absorbance at 563 nm, about 39% reduction was achieved upon the addition of 1 equivalent of cysteine and this conversion increased to 74% after a second equivalent of cysteine was added. The reduction process was driven almost to full completion with 3 equivalents of cysteine. With complex **4**, 45% reduction was achieved with 1 equivalent of cysteine, 70% with 2 equivalents and finally complete reduction with 3 equivalents of cysteine. We note that *para*-benzyl-CF<sub>3</sub> complex **6** only displayed a 32% reduction when reacted with 3 equivalents of cysteine (Fig. S4†). Interestingly, the reductions of **2** and **4** by cysteine are partially reversible as the reacted solution gradually changed from colorless back to purple upon exposure to air. The re-oxidation of **2** was accompanied by the reappearance of the d-d transition band at 563 nm. It is noteworthy that for complex **2** only ~75% regeneration was observed according to the absorbance assuming the original Cu(II) complex was reformed (Fig. S5†). Some white precipitate was observed during the process, which was identified to be free ligand by LC/MS, suggesting metal dissociation during reduction. For complex **4**, there was ~85% regeneration, but no precipitate was observed (Fig. S6†). Given the promising reactivity of **2** and **4**, further studies largely focused on these complexes.

To better understand the reaction between cysteine and complexes **2** and **4**, we used EPR to monitor the presence of paramagnetic species in solution. In agreement with the crystal structure, the room temperature EPR spectra of **2** and **4** in HEPES buffer revealed spectra consistent with square planar

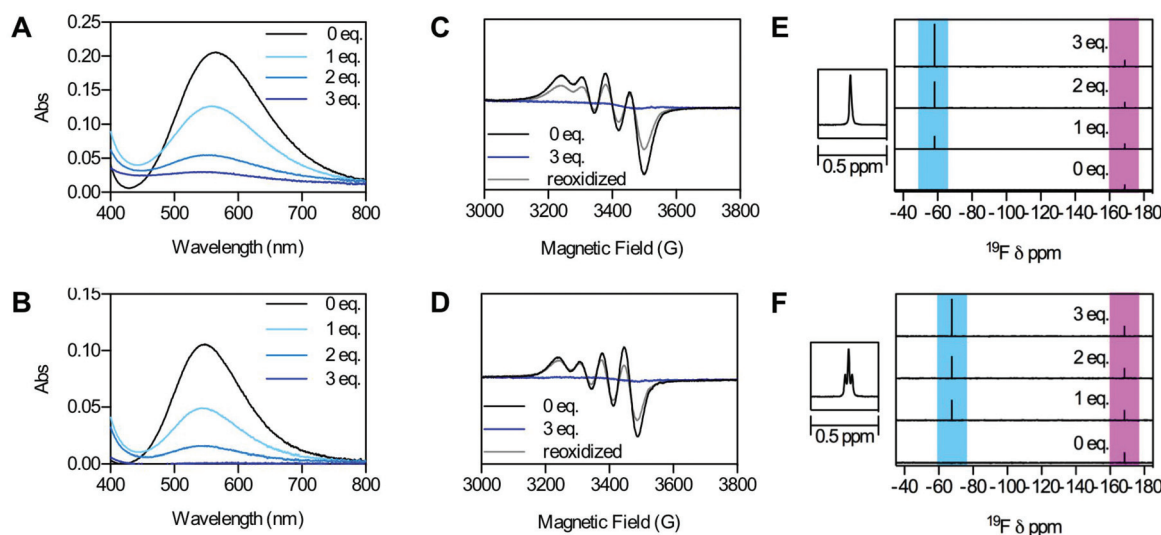


**Fig. 2** Reaction of cysteine with **2** (top row) and **4** (bottom row). (A, B) UV-vis spectra. (C, D) EPR spectra. (E, F) <sup>19</sup>F NMR spectra utilizing 5-fluorocytosine as an internal reference (pink), reduced complexes (blue). All data for **2** were obtained in 40% CH<sub>3</sub>CN in 50 mM HEPES buffer. All data for **4** were obtained in 50 mM HEPES buffer.

or octahedral geometries with elongated axial bonds.<sup>53</sup> After the addition of 3 equivalents of cysteine, full disappearance of the EPR signals was observed for both complexes, consistent with a reduction of Cu(II) to Cu(I) (Fig. 2). After exposing the reduced sample to air, the EPR signal for both complexes was partially restored. Double integration of the EPR spectra revealed a 74% signal restoration for **2** and 90% signal restoration for **4**, consistent with the percent recovery observed by UV-vis. Moreover, the EPR hyperfine features after re-oxidation perfectly matched the EPR spectra of **2** and **4**, indicating the coordination environment was maintained upon reoxidation.

NMR spectroscopy was used to further analyse the reactions between **2** and **4** with cysteine to determine the expected signal changes for <sup>19</sup>F MRI. The <sup>19</sup>F NMR spectrum of **2** displays a severely broadened peak at -52.5 ppm whereas the spectrum of **4** contained no <sup>19</sup>F peak, due to complete signal quenching in this complex. As a result, the *T*<sub>1</sub> and *T*<sub>2</sub> relaxation times of the <sup>19</sup>F nuclei in **2** and **4** could not be accurately determined and were estimated to be <0.1 ms. This signal broadening was attributed to the long electronic relaxation time (*T*<sub>1e</sub>) of Cu(II) (0.1–10 ns) and the close distance between Cu(II) and fluorine atoms in these complexes. After reacting **2** with cysteine, a sharp singlet at -58.2 ppm appeared, which is critical for higher sensitivity in <sup>19</sup>F MRI.<sup>55</sup> For complex **4** a sharp triplet at -67.5 ppm was generated upon reacting with cysteine, consistent with coupling between the CF<sub>3</sub> moiety and the adjacent methylene group. The signal intensity increased gradually as more equivalents of cysteine were introduced (Fig. 2). Moreover, this signal vanished over time upon exposure to air due to re-oxidation to Cu(II). The *T*<sub>1</sub> and *T*<sub>2</sub> relaxation times for complexes **2** and **4** after reduction were measured. For complex **2**, a *T*<sub>1</sub> of 1 s and a *T*<sub>2</sub> of 0.8 s were observed. For complex **4**, a *T*<sub>1</sub> of 0.83 s and a *T*<sub>2</sub> of 0.25 s were observed. The relatively long *T*<sub>1</sub> and *T*<sub>2</sub> relaxation times therefore allow robust <sup>19</sup>F signals to be observed after reduction.

### Mechanism of action

To determine a plausible cysteine sensing mechanism for our system, we used both NMR and UV-vis spectroscopy. The <sup>1</sup>H and <sup>19</sup>F NMR spectra of both ligand **L4** and reduced complex **4** showed excellent signal alignment, suggesting that reaction of **4** with 3 equivalents of cysteine results in formation of free ligand **L4**. Thus, we propose a reductive chelation mechanism for sensing cysteine in our system.<sup>56</sup> First, Cu(II) reacts with cysteine to form Cu(I) and cysteine radical. This is followed by formation of the cysteine disulfide and binding of Cu(I) by 2 equivalents of cysteine and removal from the cyclam scaffold (Scheme S7†). Formation of the Cu(I)-cysteine complex is accompanied by appearance of a characteristic absorbance band at 260 nm and a shoulder at 300 nm.<sup>56</sup> These bands were observed following the reaction of **2** and **4** with cysteine (Fig. S7†), consistent with the proposed mechanism. When the Cu(I) is re-oxidized in air, the cyclam ligand re-chelates the

Cu(II) and the starting complex is formed. This recovery of the starting complex was seen in UV-vis, EPR, and NMR.

### Selectivity

Selectivity of **2** and **4** towards other amino acids and reductants was further explored. Introduction of glycine, histidine, methionine, threonine, and serine resulted in no change in the Cu(II) complexes based on UV-vis spectroscopy. To further interrogate if the presence of other amino acids could affect the interaction between cysteine and water soluble **4**, an amino acid competition study was conducted. Complex **4** was incubated with 5 equivalents of various amino acids (glycine, histidine, threonine, serine, glutamic acid, aspartic acid, glutamine, asparagine, and the hydrophobic amino acids) and no reduction was observed by UV-vis. Remarkably, 3 equivalents of cysteine were still able to reduce **4** within 5 minutes even in the presence of the other amino acids (Fig. S8†). This indicates the strong binding affinity of cysteine towards **4**, which represents a valuable feature for selective cysteine detection in the complex biological environment.

As an abundant biological reductant, glutathione (GSH) plays an important role in maintaining cellular redox potential. For complex **2**, no reaction with 5 equivalents of glutathione was observed by UV-vis after 1 h. For complex **4**, only a 35% reduction was observed with 5 equivalents of glutathione after 1 h. We also tested homocysteine, another bio-reductant and biothiol, due to its structural similarity to cysteine. Partial reduction of both **2** and **4** (20% and 40% respectively) was observed with 5 equivalents of homocysteine. Nitrogen containing species NO, NaNO<sub>2</sub> and NaNO<sub>3</sub> did not reduce **2** and **4** according to UV-vis (Fig. 3). HNO, generated by using Angeli's salt, resulted in ~40% reduction of **2** and **4** after reaction of the complexes with 5 equivalents of Angeli's salt for 30 minutes. EPR revealed that the UV-vis absorbance change was probably due to ligand modification and metal displacement as strong, distinct EPR Cu(II) signals were still present after reacting **2** with 20 equivalents of Angeli's salt. Overall, complexes **2** and **4** displayed the highest reactivity with cysteine over other biological reductants.

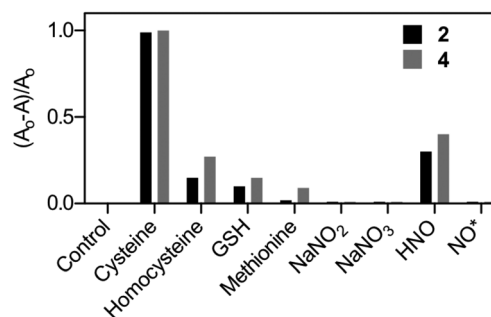


Fig. 3 Selectivity of **2** (black) and **4** (grey) with different amino acids and bioreductants. 3 equivalents of cysteine and excess NO were used. For all other reagents, 5 equivalents were used.

### $^{19}\text{F}$ magnetic resonance imaging

The capability of **2** and **4** to detect cysteine in solution by  $^{19}\text{F}$  MRI was explored using a 7 T MRI scanner. Three samples of each complex were prepared: 4 mM of Cu complex, 4 mM of Cu complex with 3 equivalents of cysteine, and 4 mM of Cu complex with 3 equivalents of cysteine exposed to air for 1 h.  $^{19}\text{F}$  MR images were acquired for the three samples using RARE pulse sequence. As expected, complexes **2** and **4** exhibit no detectable MRI signal. Conversely, when complexes **2** and **4** were reacted with cysteine, bright MRI signals were observed, with signal-to-noise ratios (SNRs) of 23 and 44, respectively. After the samples was exposed to air, the SNRs decreased to 10 and 13, respectively, which corresponds to partial re-oxidation of the complexes (Fig. 4). In order to transition into either cellular or animal studies, lower concentrations of probe are desired. A limit of detection (LOD) experiment was thus conducted to investigate the lowest concentration that can be imaged. Four different concentrations of **4** (1 mM, 0.75 mM, 0.5 mM, and 0.25 mM) were reduced by cysteine in HEPES buffer and  $^{19}\text{F}$  MR images were acquired using the same pulse sequence. A LOD of 0.3 mM was obtained by linearly fitting the SNRs *versus* concentration and assuming a lowest detectable SNR of 3.5 (Fig. S9<sup>†</sup>). To further corroborate the LOD experiment, a 0.5 mM solution of **4** was prepared in PBS buffer and 3 equivalents of cysteine (1.5 mM) were added and then exposed to air. After 20 minutes, an image was successfully acquired with an SNR of 13 for the fully reduced sample and upon exposure to air, the SNR decreased to 2 (Fig. S10<sup>†</sup>). This nicely demonstrates the capability of **4** to detect cysteine at lower probe concentration.

### Complex stability

After determining that both **2** and **4** have an efficient reactivity and selectivity toward cysteine, application in a biological system was studied. Since the solubility of **2** in water was limited, biological studies were carried out with complex **4** as

it was soluble up to 1 mM in aqueous buffer. Stability studies were conducted for **4** over the biological pH range and with different bio-available metals. With complex **4**, no change was observed over 4 days in the  $^{19}\text{F}$  NMR spectra when it was incubated with 2 equivalents of Ca(II) and Zn(II) (Fig. S11<sup>†</sup>). From pH 6–8, no change was observed in the  $^{19}\text{F}$  NMR spectrum of complex **4**. At pH 5 and 4, a  $^{19}\text{F}$  peak was observed, corresponding to less than 5% demetallation and ~20% demetallation of the complex, respectively (Fig. S12<sup>†</sup>).

### *In vitro* $^{19}\text{F}$ NMR studies

Cell studies were carried out with HeLa cells, as they are known to contain a high concentration of biothiols.<sup>34</sup> First, cytotoxicity studies were conducted (MTT assay). Cells maintained high viability in the presence of **4** at high micromolar concentrations (Fig. S13<sup>†</sup>). HeLa cells were incubated with 0.5 mM **4** for 2 hours and cell uptake of our copper complex was determined using ICP-OES. The ICP-OES data indicated that the cells contained 3.6 fmol of **4** per cell. We then looked at cells incubated under similar conditions using  $^{19}\text{F}$  NMR. We observed no peak in the  $^{19}\text{F}$  NMR spectrum of HeLa cell lysates, suggesting that cysteine levels were too low to reduce complex **4** (Fig. 4). To increase the levels of cysteine, HeLa cells were incubated with 1 mM *N*-Acetylcysteine (NAC), an external cysteine source for cells.<sup>6,57</sup> After 2 hours with NAC, the media was removed and cells were then incubated with **4**. In this case, a peak corresponding to the reduced complex appeared, indicating that the excess cysteine inside the cells was able to reduce complex **4** in this complex biological environment (Fig. 4). These results indicate that complex **4** is not toxic towards cells and can detect millimolar amounts of cysteine in biological systems.

## Conclusion

In summary, we report two Cu(II) complexes (**2** and **4**) as potential MRI probes for cysteine. Through incorporation of trifluoromethyl-benzyl or fluoroalkyl moieties on a cyclam scaffold, appropriate Cu(II/I) redox potentials can be achieved that allow their reactivities towards cysteine. The  $^{19}\text{F}$  NMR signals are effectively quenched due to the presence of Cu(II) through PRE. In solution, the Cu(II) complex reacts rapidly with cysteine and converts to a diamagnetic species with a sharp  $^{19}\text{F}$  NMR signal that was further demonstrated through  $^{19}\text{F}$  MRI. The reduction process can be conveniently reversed through exposure to air, which regenerates the Cu(II) complex. Additionally, selectivity towards other amino acids, thiols, and nitrogen containing reductants was observed. Importantly, we are able to detect excess levels of cysteine in a cellular environment using water-soluble **4**, opening up future avenues for biothiol detection using  $^{19}\text{F}$  MRI. Future work includes tuning these scaffolds to react with other bio-reductants including biologically abundant glutathione, as well as increasing fluorine density and complex stability to enable *in vivo* studies.

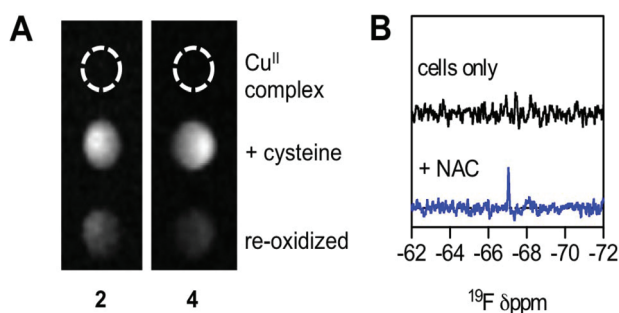


**Fig. 4** (A)  $^{19}\text{F}$  MR phantom images using RARE pulse sequence: 4 mM **2** and **4** (top), after reacting with 3 equivalents of cysteine (middle), after exposure to air for 1 h after reduction (bottom). Scanning parameters: echo time: 14.99 ms, repetition time: 1200 ms, number of acquisition: 256, rare factor: 16, matrix size:  $64 \times 64$ , field of view:  $40 \times 40 \text{ mm}^2$ , slice thickness: 50 mm. (B)  $^{19}\text{F}$  NMR after 6000 scans, top is HeLa cells with 0.5 mM of **4** and bottom is HeLa incubated with 1 mM of NAC for 2 hours and then incubated with 0.5 mM of **4**.

## Conflicts of interest

There are no conflicts to declare.

## Acknowledgements

This work was funded by start-up funds from UT-Austin (EQ), a grant from the Welch Foundation (F-1883) (EQ). We thank Dr Vincent Lynch for X-ray crystallography support, Dr Michael Rose and Dr Jonathan Sessler for providing chemicals. We also acknowledge the Imaging Research Center and Center for Electrochemistry at UT-Austin for access to their facilities. A special thanks goes to Sonya Xu and Daniel Han from the Welch Summer Scholar Program (WSSP), who helped with a portion of the synthesis and characterization. Some NMR spectra were obtained on a Bruker AVIII HD 500 that was funded by an NIH grant (Sessler PI, 1 S10 OD021508-01).

## Notes and references

- 1 L. B. Poole, *Free Radical Biol. Med.*, 2015, **80**, 148–157.
- 2 C. E. Paulsen and K. S. Carroll, *Chem. Rev.*, 2013, **113**, 4633–4679.
- 3 S. C. Lu, *FASEB J.*, 1999, **13**, 1169–1183.
- 4 R. Munday, C. M. Munday and C. C. Winterbourn, *Free Radical Biol. Med.*, 2004, **36**, 757–764.
- 5 M. Tian, F. Guo, Y. Sun, W. Zhang, F. Miao, Y. Liu, G. Song, C. L. Ho, X. Yu, J. Z. Sun and W. Y. Wong, *Org. Biomol. Chem.*, 2014, **12**, 6128–6133.
- 6 H. S. Jung, J. H. Han, T. Pradhan, S. Kim, S. W. Lee, J. L. Sessler, T. W. Kim, C. Kang and J. S. Kim, *Biomaterials*, 2012, **33**, 945–953.
- 7 S. Bannai, *Biochim. Biophys. Acta*, 1984, **779**, 289–306.
- 8 Y. M. Go and D. P. Jones, *Free Radical Biol. Med.*, 2011, **50**, 495–509.
- 9 Y. Jiang, Y. Cao, Y. Wang, W. Li, X. Liu, Y. Lv, X. Li and J. Mi, *Theranostics*, 2017, **7**, 1036–1046.
- 10 G. Liu, D. Liu, X. Han, X. Sheng, Z. Xu, S. H. Liu, L. Zeng and J. Yin, *Talanta*, 2017, **170**, 406–412.
- 11 H. Peng, W. Chen, Y. Cheng, L. Hakuna, R. Strongin and B. Wang, *Sensors*, 2012, **12**, 15907–15946.
- 12 K. Wang, H. Peng and B. Wang, *J. Cell. Biochem.*, 2014, **115**, 1007–1022.
- 13 Z. Yang, N. Zhao, Y. Sun, F. Miao, Y. Liu, X. Liu, Y. Zhang, W. Ai, G. Song, X. Shen, X. Yu, J. Sun and W. Y. Wong, *Chem. Commun.*, 2012, **48**, 3442–3444.
- 14 X. Chen, Y. Zhou, X. Peng and J. Yoon, *Chem. Soc. Rev.*, 2010, **39**, 2120–2135.
- 15 C. Zhao, K. Qu, Y. Song, C. Xu, J. Ren and X. Qu, *Chemistry*, 2010, **16**, 8147–8154.
- 16 L. Y. Niu, Y. S. Guan, Y. Z. Chen, L. Z. Wu, C. H. Tung and Q. Z. Yang, *J. Am. Chem. Soc.*, 2012, **134**, 18928–18931.
- 17 M. Zhang, M. Yu, F. Li, M. Zhu, M. Li, Y. Gao, L. Li, Z. Liu, J. Zhang, D. Zhang, T. Yi and C. Huang, *J. Am. Chem. Soc.*, 2007, **129**, 10322–10323.
- 18 G. Li, Y. Chen, J. Wu, L. Ji and H. Chao, *Chem. Commun.*, 2013, **49**, 2040–2042.
- 19 B. Liu, J. Wang, G. Zhang, R. Bai and Y. Pang, *ACS Appl. Mater. Interfaces*, 2014, **6**, 4402–4407.
- 20 L. Li and B. Li, *Analyst*, 2009, **134**, 1361–1365.
- 21 J. S. Lee, P. A. Ulmann, M. S. Han and C. A. Mirkin, *Nano Lett.*, 2008, **8**, 529–533.
- 22 J.-M. Zen, A. S. Kumar and J.-C. Chen, *Anal. Chem.*, 2001, **73**, 1169–1175.
- 23 K.-S. Tseng, L.-C. Chen and K.-C. Ho, *Electroanalysis*, 2006, **18**, 1306–1312.
- 24 A. R. Ivanov, I. V. Nazimov and L. A. Baratova, *J. Chromatogr. A*, 2000, **895**, 167–171.
- 25 S. Shahrokhian, *Anal. Chem.*, 2001, **73**, 5972–5978.
- 26 Y. S. Kim, G. J. Park, S. A. Lee and C. Kim, *RSC Adv.*, 2015, **5**, 31179–31188.
- 27 S. A. Lee, J. J. Lee, J. W. Shin, K. S. Min and C. Kim, *Dyes Pigm.*, 2015, **116**, 131–138.
- 28 M. C. Heffern, L. M. Matosziuk and T. J. Meade, *Chem. Rev.*, 2014, **114**, 4496–4539.
- 29 J. Lux and A. D. Sherry, *Curr. Opin. Chem. Biol.*, 2018, **45**, 121–130.
- 30 I. Tirotta, V. Dichiarante, C. Pigliacelli, G. Cavallo, G. Terraneo, F. B. Bombelli, P. Metrangolo and G. Resnati, *Chem. Rev.*, 2015, **115**, 1106–1129.
- 31 J. C. Knight, P. G. Edwards and S. J. Paisey, *RSC Adv.*, 2011, **1**, 1415–1425.
- 32 M. Yu, D. Xie, K. P. Phan, J. S. Enriquez, J. J. Luci and E. L. Que, *Chem. Commun.*, 2016, **52**, 13885–13888.
- 33 D. Xie, T. L. King, A. Banerjee, V. Kohli and E. L. Que, *J. Am. Chem. Soc.*, 2016, **138**, 2937–2940.
- 34 D. Xie, S. Kim, V. Kohli, A. Banerjee, M. Yu, J. S. Enriquez, J. J. Luci and E. L. Que, *Inorg. Chem.*, 2017, **56**, 6429–6437.
- 35 S. Mizukami, R. Takikawa, F. Sugihara, Y. Hori, H. Tochio, M. Wälchli, M. Shirakawa and K. Kikuchi, *J. Am. Chem. Soc.*, 2008, **130**, 794–795.
- 36 A. M. Neubauer, J. Myerson, S. D. Caruthers, F. D. Hockett, P. M. Winter, J. Chen, P. J. Gaffney, J. D. Robertson, G. M. Lanza and S. A. Wickline, *Magn. Reson. Med.*, 2008, **60**, 1066–1072.
- 37 K. L. Peterson, K. Srivastava and V. C. Pierre, *Front. Chem.*, 2018, **6**, 160.
- 38 K. Srivastava, E. A. Weitz, K. L. Peterson, M. Marjańska and V. C. Pierre, *Inorg. Chem.*, 2017, **56**, 1546–1557.
- 39 L. A. Basal, M. D. Bailey, J. Romero, M. M. Ali, L. Kurenbekova, J. Yustein, R. G. Pautler and M. J. Allen, *Chem. Sci.*, 2017, **8**, 8345–8350.
- 40 A. A. Kislukhin, H. Xu, S. R. Adams, K. H. Narsinh, R. Y. Tsien and E. T. Ahrens, *Nat. Mater.*, 2016, **15**, 662–668.

- 41 K. H. Chalmers, A. M. Kenwright, D. Parker and A. M. Blamire, *Magn. Reson. Med.*, 2011, **66**, 931–936.
- 42 A. M. Kenwright, I. Kuprov, E. D. Luca, D. Parker, S. U. Pandya, P. K. Senanayake and D. G. Smith, *Chem. Commun.*, 2008, 2514–2516.
- 43 Z. X. Jiang, Y. Feng and Y. B. Yu, *Chem. Commun.*, 2011, **47**, 7233–7235.
- 44 M. Yu, B. S. Bouley, D. Xie, J. S. Enriquez and E. L. Que, *J. Am. Chem. Soc.*, 2018, **140**, 10546–10552.
- 45 P. Harvey, I. Kuprov and D. Parker, *Eur. J. Inorg. Chem.*, 2012, **2012**, 2015–2022.
- 46 I. Bertini, C. Luchinat, G. Parigi and R. Pierattelli, *ChemBioChem*, 2005, **6**, 1536–1549.
- 47 T. J. Wadas, E. H. Wong, G. R. Weisman and C. J. Anderson, *Chem. Rev.*, 2010, **110**, 2858–2902.
- 48 L. E. McQuade and S. J. Lippard, *Inorg. Chem.*, 2010, **49**, 7464–7471.
- 49 S. Kim, M. A. Minier, A. Loas, S. Becker, F. Wang and S. J. Lippard, *J. Am. Chem. Soc.*, 2016, **138**, 1804–1807.
- 50 J. Blahut, K. Bernášek, A. Gálisová, V. Herynek, I. Císařová, J. Kotek, J. Lang, S. Matějková and P. Hermann, *Inorg. Chem.*, 2017, **56**, 13337–13348.
- 51 J. Blahut, P. Hermann, A. Gálisová, V. Herynek, I. Císařová, Z. Tošner and J. Kotek, *Dalton Trans.*, 2016, **45**, 474–478.
- 52 S. L. Hart, R. I. Haines, A. Decken and B. D. Wagner, *Inorg. Chim. Acta*, 2009, **362**, 4145–4151.
- 53 A. E. Goeta, J. A. Howard, D. Maffeo, H. Puschmann, J. A. G. Williams and D. S. Yufit, *J. Chem. Soc., Dalton Trans.*, 2000, 1873–1880.
- 54 C. Amatore, J.-M. Barbe, C. Bucher, E. Duval, R. Guilard and J.-N. Verpeaux, *Inorg. Chim. Acta*, 2003, **356**, 267–278.
- 55 C. Jacoby, S. Temme, F. Mayenfels, N. Benoit, M. P. Krafft, R. Schubert, J. Schrader and U. Flögel, *NMR Biomed.*, 2014, **27**, 261–271.
- 56 L. Pecci, G. Montefoschi, G. Musci and D. Cavallini, *Amino Acids*, 1997, **13**, 355–367.
- 57 M. Mayer and M. Noble, *Proc. Natl. Acad. Sci. U. S. A.*, 1994, **91**, 7496–7500.